Cellular Physiology and Biochemistry

Cell Physiol Biochem 2015;35:1943-1957
DOI: 10.1159/000374003
Published online: March 27, 2015
Accepted: January 20, 2015

1421-9778/15/0355-1943$39.50/0

Original Paper

The Anticancer Activity of the Substituted Pyridone-Annelated Isoindigo (5'-Cl) Involves G0/G1 Cell Cycle Arrest and Inactivation of CDKs in the Promyelocytic Leukemia Cell Line HL-60

Ayman M. Saleh[a,b] Ahmad Aljada[a,b] Mustafa M. El-Abadelah[c] Mutasem O. Taha[d] Salim S. Sabri[c] Jalal A. Zahra[c] Mohammad Azhar Aziz[b]

[a]Department of Basic Medical Sciences, College of Medicine, King Saud Bin Abdulaziz University for Health Sciences (KSAU-HS), National Guard Health Affairs, Riyadh, Kingdom of Saudi Arabia, [b]King Abdullah International Medical Research Center (KAIMRC), National Guard Health Affairs, Riyadh, Kingdom of Saudi Arabia, [c]Department of Chemistry, Faculty of Science, The University of Jordan, Amman, Jordan, [d]Department of Pharmaceutical Sciences, Faculty of Pharmacy, The University of Jordan, Amman, Jordan

Key Words
Pyridone-annelated isoindigo • Anticancer compound • Cell cycle • G0/G1 phase • Cyclin-D • CDK2 • CDK4 • Rb • Kinase activity • HL-60 cell line

Abstract
Background/Aims: The antileukemic potential of isoindigos make them desired candidates for understanding their mechanism of action. We have recently synthesized a novel group of pyridone-annelated isoindigos and identified the derivative 5'-Cl that is cytotoxic to various cancer cell lines. In the present study, we analyzed the effect of this compound on cell cycle of the promyelocytic leukemia cell line HL-60. ***Methods:*** HL-60 cells were treated with 5'-Cl and its effect on cell cycle stages were determined by flow cytometry. Expression of cyclins, cyclin dependent kinases (CDKs) and cyclin kinase inhibitors (CKIs) were determined by Western blotting, and activation of CDKs was studied using kinase assays. ***Results:*** 5'-Cl remarkably arrested cell cycle in HL-60 cells at the G0/G1 phase in a dose and time-dependent manner. Furthermore, 5'-Cl treatment significantly inhibited expression of D-cyclins, CDK2 and CDK4 and suppressed phosphorylation of the retinoblastoma protein Rb, whereas it increased the level of CKI p21. Molecular modelling experiments show that 5'-Cl may compete with ATP for binding to the catalytic subunit of CDK2 and CDK4 that could lead to inhibition of these enzymes. Indeed, 5'-Cl inhibited the kinase activity of CDK2 and CDK4 both in cell free systems and in treated cells. 5'-Cl also inhibited cell cycle progression in several other tumor cell lines. ***Conclusion:*** We demonstrate the potent inhibitory effects of 5'-Cl on HL-60 cells could be mediated by arresting cells in the G0/G1 phase.

Ayman M. Saleh

College of Medicine, King Saud Bin Abdulaziz University for Health Sciences (KSAU-HS) and King Abdullah International Medical Research Center (KAIMRC), National Guard Health Affairs, P.O. Box: 3660, Mail Code: 3127, Riyadh11481 (Kingdom of Saudi Arabia)
E-Mail salehay@ksau-hs.edu.sa or salehay@ngha.med.sa

Introduction

Tumor cells are characterized by having a deregulated cell cycle which contributes to their uncontrolled proliferation (reviewed in [1, 2]). The molecular mechanisms of cell cycle arrest by many anticancer agents involve modulation of several cell cycle regulatory proteins. In eukaryotes, the cell cycle is controlled through the sequential activation and inactivation of cyclin-dependent kinases (CDKs) that drive cell cycle progression through phosphorylation/dephosphorylation of several regulatory factors [1, 3]. Activation of CDK requires its association with specific cyclins and their phosphorylation at a conserved threonine residue by CDK-activating kinase (CAK) [1]. Inactivation of CDK-cyclin complex is also triggered by phosphorylation of another a conserved threonine/tyrosine amino acids of the kinase or binding of the complex to CDK inhibitory factors (CKIs) [4, 5].

Transition from G1 to S phase in mammalian cells requires increased levels of cyclins D, E and A, which bind to and promote activation of the catalytic subunits of CDK2, CDK4 and CDK6 [6]. The retinoblastoma tumor suppressor (Rb) is an essential target protein that is phosphorylated by these CDK–cyclin complexes [7, 8]. Hyperphosphorylation of Rb inactivates its function and dissociates the E2F transcription factor from Rb, which activates transcription of components of the DNA replication machinery, thereby committing the cell to S phase of the cell cycle [8-10].

CDK activity can be counteracted by CKIs, which bind to CDK alone or to the CDK/cyclin complex and regulate CDK activity. Two classes of these inhibitors have been described so far. The first one ($p16^{INK4a/CDKN2A}$, $p15^{INK4b}$, $p18^{INK4c}$ and $p19^{INK4d}$) is specific for Rb kinases, i.e. CDK4 and CDK6 [5]. The second class ($p21^{WAF1/CIP1}$, $p27^{Kip1}$ and $p57^{Kip2}$) has a broader range of activity and inhibits most of the known CDK/cyclin complexes, but with a preference for CDK2/cyclin and Cdk4/cyclin complexes [5]. CKIs are regulated both by internal and external signals: the expression of $p21^{WAF1/CIP1}$ is under transcriptional control of the p53 tumor suppressor [11, 12]. The *p53* gene is the most commonly mutated gene in human cancer, and regulation of $p21^{WAF1/CIP1}$ in response to DNA damage is lost when p53 is inactivated [11-13]. However, the expression of *p21* in a variety of tissues from p53-null mice suggests that it is also regulated by a p53-independent mechanism [14].

Bis-indole containing alkaloids Indigo, indirubin and isoindigo have been studied for their anticancer properties. There are several natural resources for these alkaloids. [15]. While indigo is mainly used as a textile dye, indirubin was identified as the active ingredient of a traditional Chinese recipe (Danggui Longhui Wan) used for treatment of chronic myelogenous leukemia (CML) [16, 17]. Indirubin exerts its antileukemic effect through multi-signaling pathways including inhibition of DNA biosynthesis and assembly of microtubules, arresting cell cycle at G1 phase, interaction with the aryl hydrocarbon receptor (AhR) and down-regulation of *c-myb* gene expression [17-21]. The impairment of cell cycle progression in CML cells by Indirubin is mediated by the ability of the compound to compete with ATP for binding to the catalytic subunit of CDKs, leading to inhibition of these enzymes [22, 23]. However, indirubin could cause severe gastrointestinal side effects due to the poor water solubility, and may lead to bone marrow suppression and drug-resistance in prolonged treatments [17]. To overcome the solubility problems, Meisoindigo (1-methyl isoindigo) was developed and subjected to clinical trials [17, 24], and is used as an indirubin substitute for treatment of CML in China [24].

Recently, there have been efforts to synthesize novel induribin and isoindigo derivatives with improved bioavailability and anticancer efficacies. Several of these compounds have been shown to inhibit CDKs and glycogen-synthase kinase (GSK-3β) and induce apoptosis in leukemic cells with varying degrees of potency [17-20, 22, 23, 25-28]. In spite of extensive investigations on the mode of action of isoindigos in various malignancies, comprehensive study is yet to be done.

With an aim to synthesize more soluble and effective anticancer isoindigo derivatives, we recently reported the synthesis of a novel series of pyridone-annelated isoindigo and evaluated their antitumor activities against various cancer cell lines [29]. Our analysis

Chart 1. Chemical Structure of 5'-Cl compound. [(*E*)-1-(5'-Chloro-2'-oxoindolin-3'-ylidene)-6-ethyl-2,3,6,9-tetrahydro-2,9-dioxo-1*H*-pyrrolo[3,2-*f*]quinoline-8-carboxylic acid].

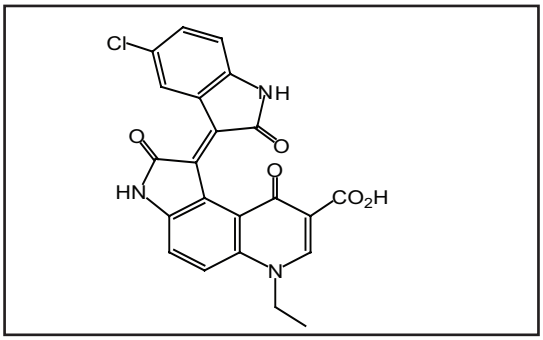

have identified a compound [(*E*)-1-(5'-Chloro-2'-oxoindolin-3'-ylidene)-6-ethyl-2,3,6,9-tetrahydro-2,9-dioxo-1*H*-pyrrolo[3,2-*f*]quinoline-8-carboxylic acid] (known here as the 5'-Cl compound, Chart 1) which effectively inhibits the proliferation of different human hematological and solid tumor derived cell lines in a selective manner [29]. Our results show that 5'-Cl induces a caspase-dependent and independent apoptosis, and triggers dysfunctioning of mitochondria in the human acute myelogenous leukemia cell line HL-60 [30].

In this report, we further characterize the antiproliferative mechanisms of 5'-Cl and reveal that the compound can inhibit the proliferation of HL-60 cells through G0/G1 phase arrest, mediated by modulating the expression and function of the G1 phase-related proteins. Furthermore, we show that 5'-Cl inhibits the kinase activities of CDK2 and CDK4 both in cell free systems and in treated HL-60 cells. Molecular modelling studies corroborate the results of kinase assays that 5'-Cl shows competitive inhibition of CDK2 and CDK4.

Materials and Methods

Reagents

The pyridone-annelated isoindigo 5'-Cl [[(*E*)-1-(5'-Chloro-2'-oxoindolin-3'-ylidene)-6-ethyl-2,3,6,9-tetrahydro-2,9-dioxo-1*H*-pyrrolo[3,2-*f*]quinoline-8-carboxylic acid] was previously synthesized and chemically characterized in our study [29]. Components of lysis, immunoprecipitation and kinase buffers, protease inhibitors (PMSF, pepstatin A, leupeptin, and aprotinin) were acquired from Sigma Aldrich (St Louis, Missouri, USA). All cell lines used in this study were obtained from American Type Culture Collection (ATCC; Manassas, Virginia, USA). Cell culture media (RPMI 1640 and DMEM), penicillin-streptomycin, trypsin, phosphate buffer saline (PBS), and heat inactivated fetal bovine serum (FBS) were purchased from Invitrogen (Invitrogen, Carlsbad, California, USA). The polyclonal or monoclonal antibodies against cell cycle regulators were obtained from Cell Signaling (Beverly, Massachusetts, USA).

Cell culture conditions

HL-60 (acute promyelocytic leukemia, ATCC® CCL-240™), K562 (chronic myelogenous leukemia,ATCC® CCL-243™) and THP-1 (acute monocytic leukemia, ATCC® TIB-202™) cells were maintained in RPMI-1640, while HepG2 (hepatocellular carcinoma, ATCC® HB-8065™), MCF7 (human breast adenocarcinoma, ATCC® HTB-22™) and Caco-2 (human colorectal adenocarcinoma, ATCC® HTB-37™) cells were cultured in DMEM medium. The media were supplemented with 10% (v/v) heat inactivated FBS, penicillin G (100U/mL) and streptomycin (100 mg/mL), and cells were incubated at 37°C in a 5% CO_2/95% humidified incubator. Cells were seeded at an appropriate density according to each experimental design.

Flow cytometric analysis of cell cycle

Distribution of cells in different stages of cell cycle was analyzed by flow cytometry using the Muse™ Cell Cycle Kit from EMD Millipore Bioscience (Darmstadt, Germany). The kit utilizes propidium iodide (PI) staining to allow quantitative measurements of percentage of cells in the G0/G1, S and G2/M phases on the Muse™ Cell Analyzer (EMD Millipore Bioscience). The cell cycle analysis was performed according to the manufacturer's protocol, and as recently described [31]. Briefly, exponentially growing HL-60 cells (5

× 10^5 cells/mL) were treated with different concentrations of 5'-Cl (0.0 to 8.0 μM) for 24h or with 4.0 μM for various periods of time (0 to 48h). After incubation, 1 × 10^6 cells were harvested and washed with PBS, followed by fixation with ice-cold 70% ethanol at −20°C for 3h. The cells were then washed with PBS, stained with 200 μL of PI/RNAse reagent for 30 min and analyzed by the Muse™ Cell Analyzer. Adherent cells were trypsinized after treatment, washed once with PBS, and fixed in 70% ethanol overnight at −20°C before analysis as described above. All the compound stock solutions were prepared in a solvent containing 50% DMSO and 50% PBS. Therefore, the control cells were treated with equal amount of the carrier solvent (0.05% DMS0), and showed no effect on cell cycle when compared with the solvent-free control cells. Under similar conditions, cells were treated with 0.02 μM and 0.04 μM cytarabine as internal controls to validate the assay results (data not shown).

CDK2 and CDK4 kinase assay in cell-free systems and cultured cells

Kinase assays were performed on HL-60 as previously described [32-34], with some modifications. For *in vitro* CDKs kinase assay, exponentially growing untreated HL-60 cells were lysed for 30 min at 4°C in a buffer containing [50 mM Tris (pH 7.5), 10% glycerol, 150 mM NaCl, 0.5% NP-40, 50 mM NaF, 1 mM Na_3VO_4, 1 mM DTT, 1 mM EGTA, 5 mM EDTA, 1 mM phenylmethylsulfonyl fluoride (PMSF), 2 μg/mL of each pepstatin A, aprotinin and leupeptin, and phosphatase inhibitor cocktail I and II (Calbiochem, California, USA). The cell debris was removed by centrifugation at 12,000 *g* for 10 min at 4°C. Protein lysates were pre-cleared twice with 50 μL protein A/G plus-agarose beads (Santa Cruz Biotechnology, Santa Cruz, California, USA). 4 mg of total protein was incubated with anti-CDK2 or anti-CDK4 antibody and protein A/G plus agarose for 12h at 4°C. The immunoprecipitate was washed three times with the above buffer and twice with a kinase buffer containing [50 mM HEPES (pH 7.0), 10 mM $MgCl_2$, 5 mM $MnCl_2$, 1 mM DTT, 5 μM ATP] and separated into 10 tubes. The kinase reactions were done in a final volume of 40 μL kinase buffer containing 2 μg histone H1 (for CDK2; Calbiochem) or 1 μg Gst-Rb (for CDK4; Santa Cruz Biotechnology) substrates, various concentrations of the test compound and 5 μCi [γ-^{32}P]ATP (3000 Ci/mmol, PerkinElmer Inc., Waltham, Massachusetts, USA), and carried out for 30 min at 30°C. SDS sample buffer was then added. The mixtures were boiled for 5 min, and separated on 12% polyacrylamide gels. The gels were dried, visualized by autoradiography, and quantitated by densitometry (using the UN-SCAN-IT 7.0 gel and graph digitizing software, Silk Scientific, Inc., Orem, Utah, USA). The concentration of test compound leading to 50% inhibition of the kinase activity (IC_{50}), compared to untreated control, was determined from the sigmoidal curve obtained by plotting the percentages of band intensity relative to the control versus logarithmic concentration of test compound using a non-linear regression analysis of GraphPad Prism 6 (GraphPad Software, San Diego, California, USA).

For *in vivo* CDKs kinase assay, HL-60 cells (2 x 10^5) were seeded in 100 mm plastic culture dishes for 24h and treated with different concentrations of 5'-Cl (0 to 8.0 μM) for 24h or with a fixed concentration of 4.0 μM for various periods of time ranging from 0 to 48h. Cell lysis preparation and immunoprecipitation were performed as described above. Kinase assay was carried out in 50 μL kinase buffer containing CDK2- or CDK4-immunoprecipitates from 300 μg of protein lysate. Before addition of the radioactive ATP, 10 μL of the slurry was removed from each sample to separate tubes for Western blot analysis of the immunoprecipitated CDK, to verify that equal amount of the desired CDK is present in each sample. To the remaining 40 μL, 5 μCi [γ-^{32}P]ATP were added to each reaction tube and the kinase assay was performed as described above.

Western blot analysis

5'-Cl-treated and untreated HL-60 cells were harvested by centrifugation at 500 *g*, washed twice with PBS, and suspended in a lysis buffer containing 100 mM HEPES, pH 7.4, 10% sucrose, 10 mM DTT, 0.1% CHAPS, 150 mM NaCl, and protease inhibitors (1 mM PMSF and 2 μg/mL each leupeptin, aprotinin, and pepstain A). The cells were lysed by six repeated cycles of freeze/thawing (in dry ice/37°C water bath) and then centrifuged at 4°C for 30 min at 14,000 *g*. The supernatant was collected and stored at −80°C or used immediately. Total protein was measured using Bradford reagent (Bio-Rad Laboratories Inc., California, USA). Protein samples (50 μg/well) were separated on 12% SDS–polyacrylamide gels and electroblotted onto a PVDF membrane (Millipore Corp., Massachusetts, USA). All primary antibodies were purchased from Cell Signaling Technology; for cyclin D1, D2, D3 and E were obtained from (cyclin antibody sampler kit, catalogue # 9869), for CDK2, CDK4, CDK6, p21 and p27 (from cell cycle regulation antibody sampler kit, catalogue # 9932), and for Rb and phospho-Rb (from cell cycle check point kit, catalogue # 9917). In all gels, pre-stained protein molecular weight markers (Santa Cruz Biotechnology) were included. The blots were

also immuneprobed with a rabbit polyclonal antibody against the cytoskeletal protein α-tubulin (Santa Cruz Biotechnology).

Docking study

Preparation of CDK2 and CDK4 crystal structures: The 3D coordinates of the two proteins were retrieved from the Protein Data Bank (CDK2 PDB code: 4ERW, resolution 2.0 Å; CDK4 PDB code: 1GIH, resolution 2.8 Å). Hydrogen atoms were added to the protein utilizing DiscoveryStudio 2.5.5 templates for protein residues. Gasteiger-Marsili charges were assigned to the protein atoms as implemented within DiscoveryStudio 2.5.5 (Accelrys Inc., San Diego, California, USA) as described in [35].

Protein structures were utilized in subsequent docking experiments without energy minimization. Explicit water molecules were kept. Docking experiment was conducted employing LigandFit docking engine [36, 37]. There are two steps implemented in the LigandFit process:

(1) Defining the location(s) of potential binding site. In the current docking experiments the binding site was generated from the co-crystallized ligands within targeted proteins.

(2) Docking the ligands in the binding site. In LigandFit, docking is composed of few substeps: (i) Conformational search of flexible ligands employing Monte Carlo randomized process. (ii) Pose/conformation selection based on shape similarity with the binding site. (iii) Candidate conformers/poses exhibiting low shape discrepancy are further enrolled in calculation of the dock energies. (iv) Each docked conformation/pose is further fitted into the binding pocket through a number of rigid-body minimization iterations. (v) Docked conformers/poses that have docking energies below certain user-defined threshold are subsequently clustered according to their RMS similarities. Representative conformers/poses are then selected, further energy-minimized within the binding site, and saved for subsequent scoring.

Statistical analysis

Data presented are the means ± SD of results from a minimum of three independent experiments with similar patterns. Statistical analysis was performed using one-way ANOVA, and Tukey-Kramer multiple-comparison test was performed by using GraphPad Prism 6 software. A $p < 0.05$ value was considered statistically significant.

Results

5'-Cl induces cell cycle arrest in the G0/G1 phase of HL-60 cells

We examined the effect of 5'-Cl compound on cell cycle progression, using flow cytometry analysis after staining the treated HL60 cells with PI. When cells were treated with increasing concentrations of 5'-Cl for 24h, the dose-dependent cell cycle arrest at G0/G1 phase was evident with a concomitant decrease in the S and G2/M phase (Fig. 1A). The percentage of HL-60 cell population in G0/G1 phase increased from 40.30 ± 3.68% (untreated control) to 69.11 ± 2.42% after incubation with 8.0 μM of 5'-Cl in a dose-dependent manner. S-phase cells showed slightly significant decrease, after exposure to 8.0 μM, but the percentage of G2/M-phase cells decreased dramatically from 28.43 ± 2.72% in the untreated control to 8.14 ± 2.93% in the cells treated with 8.0 μM of 5'-Cl. These results indicate that growth inhibitory effects of 5'-Cl involve cell cycle arrest at G1 phase in a dose-dependent manner. In addition, the cell cycle arrest induced by this compound showed a time-dependent pattern (Fig. 1B). A significant increase in the cell population at G0/G1 was evident after incubating with 4.0 μM of 5'-Cl for 6h (from 41.42 ± 1.95% to 48.23 ± 2.36, compared to control at 0h), and reached 73.18 ± 2.91% after 48h of treatment.

5'-Cl modulates the expression of cell-cycle-regulatory proteins in HL-60 cells

To determine the molecular mechanism of cell-cycle arrest in the G0/G1 phase, we examined whether or not the effects induced by 5'-Cl were associated with changes in the level of G1-S transition-regulatory factors. After treating HL-60 cells with increasing concentrations of 5'-Cl, we observed a dose-dependent decrease in the levels of cyclin D1, D2 and D3 (Fig. 2A). The reduction in cyclin D protein levels was accompanied by a

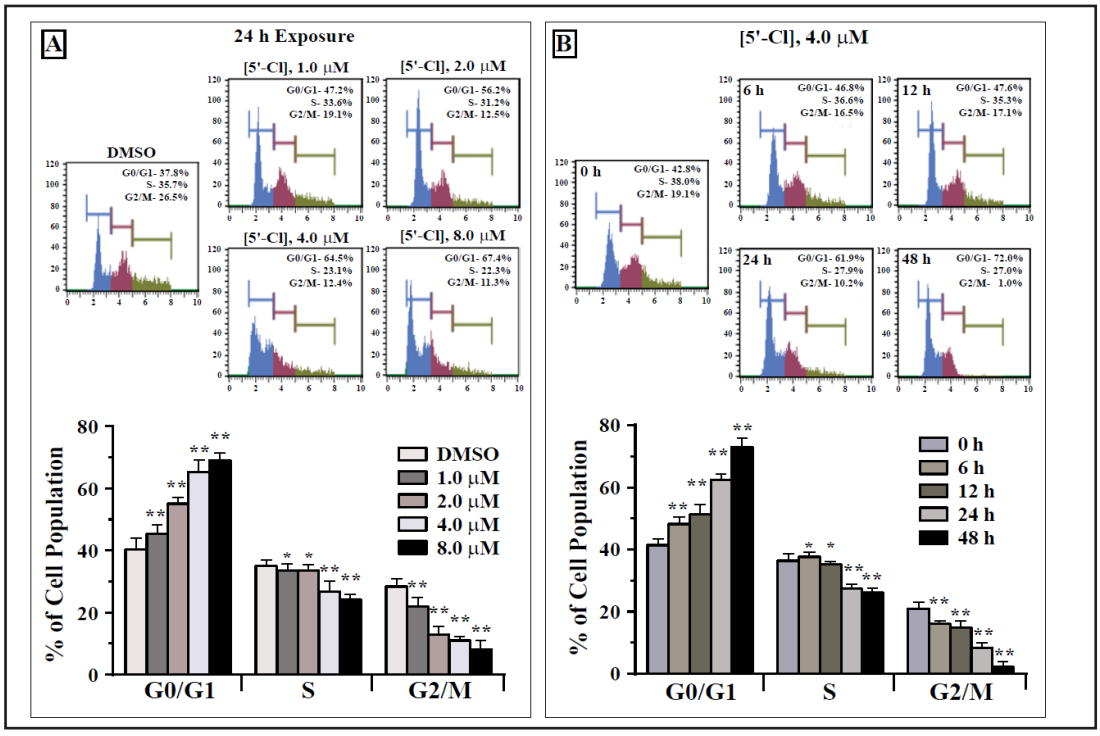

Fig. 1. 5'-Cl induces a dose and time-dependent cell cycle arrest at G0/G1 phase in HL-60 cells. (A) HL60 cells were treated with DMSO (0.05%) or increasing concentrations of 5'Cl (1.0 to 8.0 μM) for 24 h. (B) Similarly, HL-60 cells were treated with a fixed concentration of 4.0 μM 5'-Cl for the indicated periods, and cell cycle analysis was done as described under the methods. Data shown are representative of three independent experiments. The bar graphs show the mean ± SD of the three independent experiments. (**) For values that are significantly different and (*) for statistically insignificant when compared to untreated control.

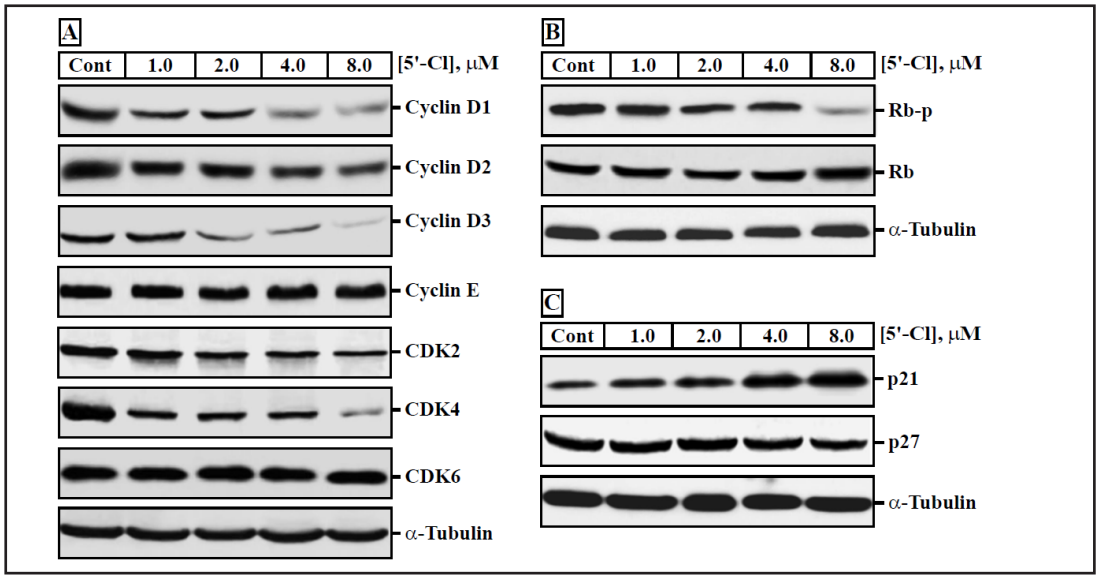

Fig. 2. 5'-Cl modulates the expression of D-type cyclins, CDK2, CDK4 and p21, and reduces the phosphorylation of Rb. HL60 cells were treated with 0.05% DMSO (control) or increased concentrations of 5'-Cl (1.0 μM to 8.0 μM) for 24 h, then 50 μg proteins were analyzed by Western blotting with antibodies against different cyclins and CDKs (A), Rb and phospho-Rb (B), and p21 and p27 (C). The immunoblots shown are representations of two independent experiments. The same membranes were also probed with an antibody against α-tubulin as loading controls.

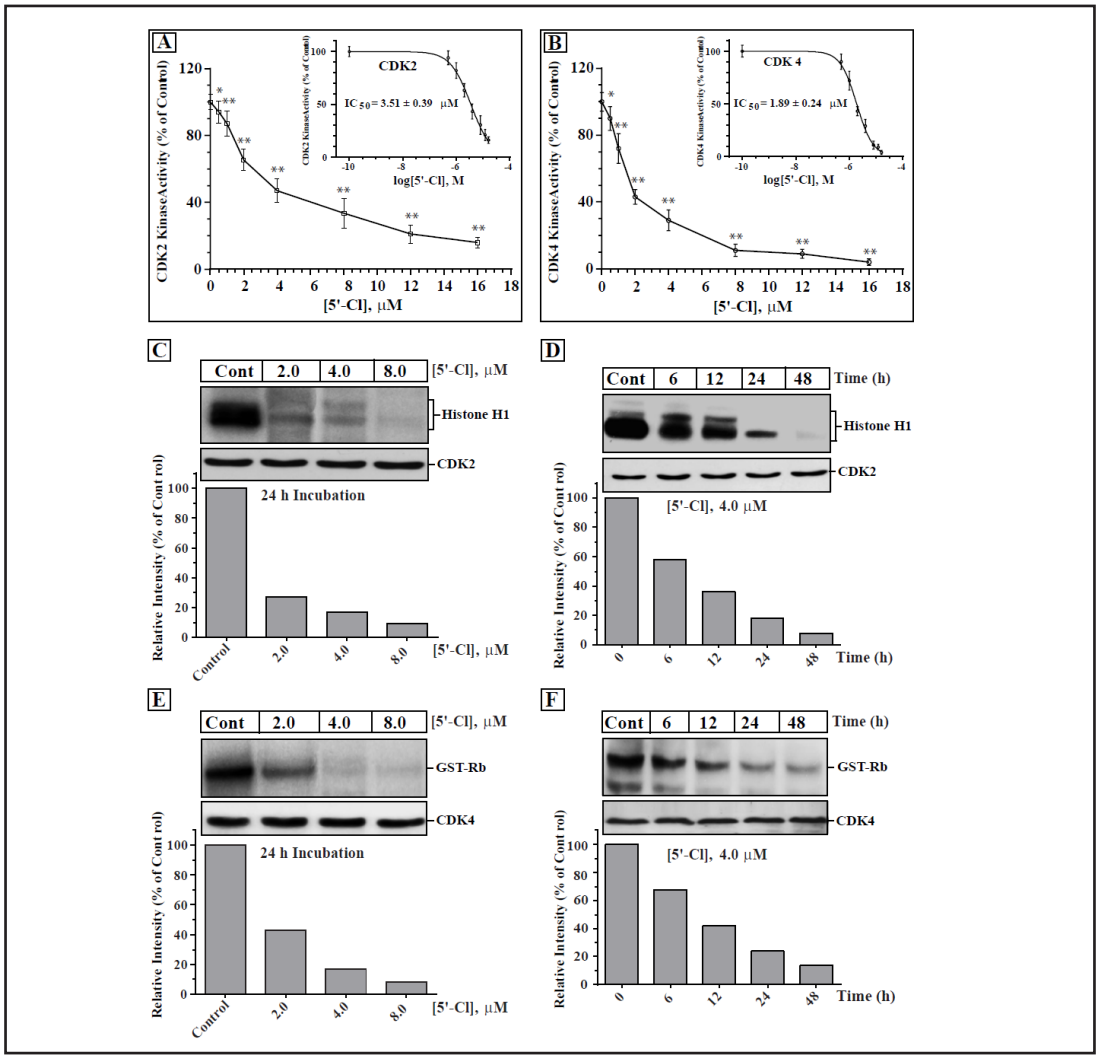

Fig. 3. 5'-Cl inhibits the kinase activities of CDK2 and CDK4 in cell-free system and cultured HL-60 cells. CDK2 (A) and CDK4 (B) immunoprecipitated complexes were prepared from exponentially growing untreated cells, and reacted with [γ-^{32}P]ATP in the presence of histone H1 (for CDK2, A) and GST-Rb (for CDK4, B) substrates and increasing concentrations of 5'-Cl for 30 min at 30°C. Quantification of the histone H1 and GST-Rb-phosphorylated forms was performed by densitometric analysis, and the IC_{50} was calculated using a non-linear regression analysis of GraphPad Prism 6 (upper right corner). Data represent the means ± SD of three independent experiments. (**) For values that are significantly different and (*) for statistically insignificant when compared to untreated control. (C and E) HL-60 cells were treated with various concentrations of 5'-Cl (0.0 to 8.0 µM) for 24 h, or with a fixed concentration of 4.0 µM for increasing periods (D and F). Total cell lysates were used for immunepreciptation, and the kinase activities were assayed with histone H1 (C and D, for CDK2) and GST-Rb (E and F, for CDK4) as substrates. The experiments were performed as described under methods. Data shown are representative of two independent experiments. The bar graphs represent the mean of the densitometric intensities of the visualized bands. The same immunoprecipitates were also immunoblotted with CDK2 (C and D) and CDK4 (E and F) to verify equal amounts of the desired CDK was present in each sample.

concentration-dependent decrease in the amount of CDK2 and CDK4 (Fig. 2A). On the other hand, the expression patterns of cyclin E and CDK6 were not significantly affected in the same treatments.

Rb is one of the most relevant targets of CDKs in cell cycle control [7, 9, 38], Therefore, to examine the effect of 5′-Cl on the phosphorylation status of this protein. Our results showed a

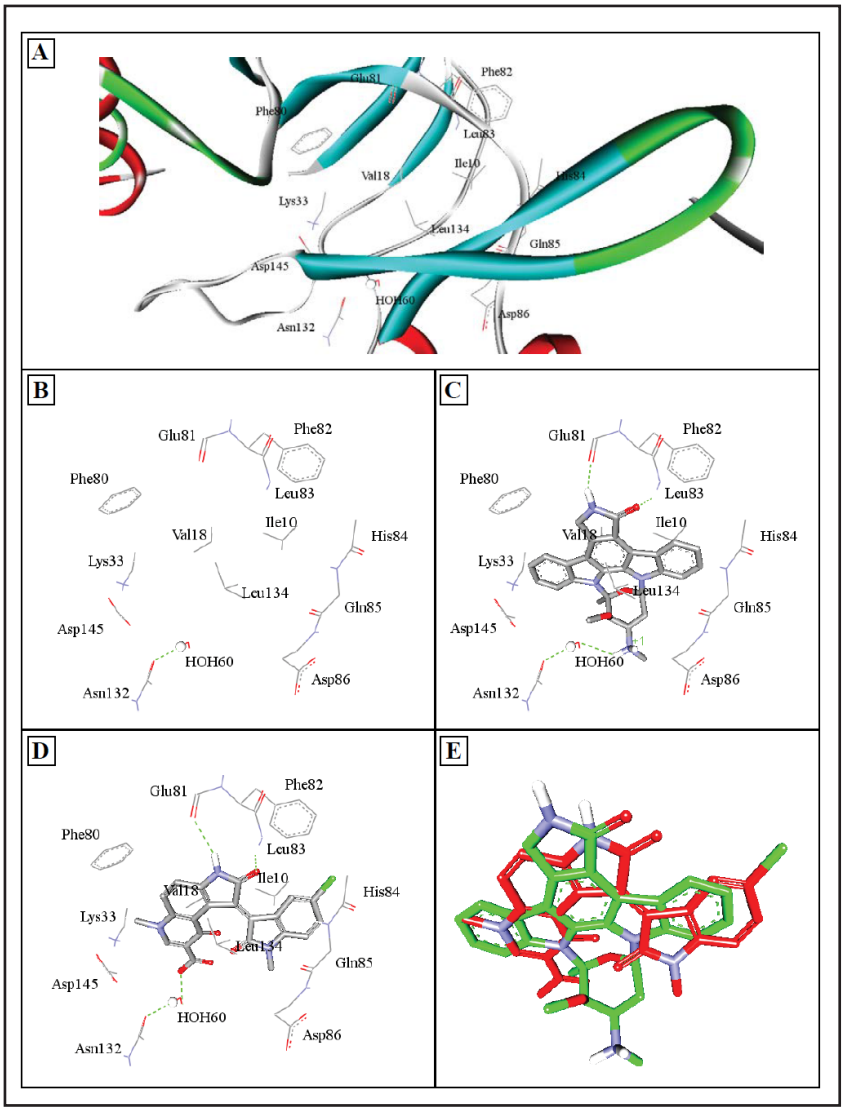

Fig. 4. Molecular docking of 5'-Cl within the ATP binding pocket of CDK2. (A) Panoramic view of the X-ray crystallographic structure of the binding pocket of CDK2 kinase domain (PDB code: 4ERW, resolution 2.0 Å). (B) Detailed view of CDK2 kinase binding pocket showing amino acids involved in binding. (C) X-ray crystallographic structure of staurosporine co-crystallized within the binding pocket of CDK2 kinase. (D) Docked structure of 5'-Cl within CDK2. (E) Superposition of the co-crystallized structure of staurosporine (green) over 5'-Cl docked structure (red).

significant dose-dependent decrease in the level of phospho-Rb, while the expression of total Rb remained almost unchanged (Fig. 2B). Moreover, 5'-Cl was able to elicit a dose-dependent increase in protein levels of CDK inhibitor p21, but not in p27 (Fig. 2C).

Effect of 5'-Cl on the activities of CDK2 and CDK4 in a cell-free system and cultured HL-60 cells

To examine whether 5'-Cl would directly inhibit CDK2 and CDK4 in HL-60 cells, we first measured the effect of the compound on the kinase activities of these CDKs in cell-free systems. As shown in Fig. 3A and 3B, 5'-Cl was able to inhibit both CDK2 and CDK4 in a concentration-dependent manner, with an approximate IC_{50} of ~3.51 ± 0.39 μM and ~1.89 ± 0.24 μM, respectively. We next evaluated the kinase activities of CDK2 and CDK4 from 5'-Cl-treated HL-60 cells. As shown in Fig. 3C and 3E, the kinase activities of both CDK2 and CDK4 were inhibited in a dose-dependent manner, and >90% of the substrates phosphorylation status were inhibited compared with untreated control cells after incubation with 8.0 μM of 5'-Cl. The inhibition of CDK2 and CDK4 kinase activities were also time-dependent in cultured HL-60 cells (Fig. 3D and 3F). The kinase activities of both CDKs were inhibited by increasing the incubation period with the compound, and reached 80-85% loss in the activities after 24h treatment.

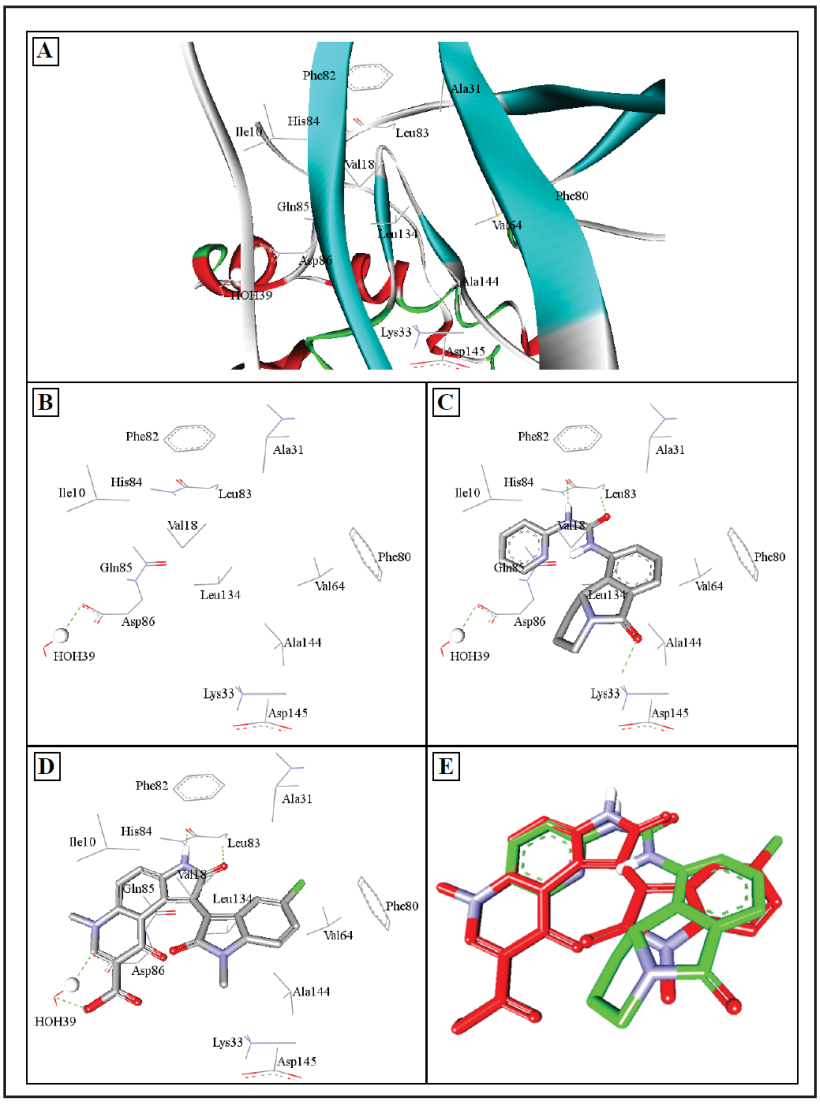

Fig. 5. Molecular docking of 5'-Cl within the ATP binding pocket of CDK4. (A) Panoramic view of the X-ray crystallographic structure of the binding pocket of CDK4 mimic of CDK2 kinase domain (PDB code: 1GIH, resolution 2.8 Å). (B) Detailed view of CDK4 kinase binding pocket showing amino acids involved in binding. (C) X-ray crystallographic structure of co-crystallized ligand (PDB code: 1PU501) within the binding pocket of CDK4. (D) Docked structure of 5'-Cl within CDK4. (E) Superposition of the co-crystallized ligand (green) over 5'-Cl docked structure (red).

Docking studies

The potent inhibitory effects of 5'-Cl against CDK2 and CDK4, prompted us to dock this compound into the binding pockets of both proteins and compare its optimal docked poses with the co-crystallized poses of corresponding potent ligands. Fig. 4 compares how the potent CDK2 inhibitor, staurosporine, binds within CDK2 kinase binding pocket (PDB code: 4ERW, resolution 2.0 Å) (Fig. 4A and 4B) with the way 5'-Cl docks into the binding pocket of the same protein. The 2-pyrrolidone of staurosporine and the 2-indolone of 5'-Cl share similar hydrogen bonding pattern with the peptidic NH of Leu83 and the peptidic carbonyl of Glu81. Similarly, both staurosporine and 5'-Cl are hydrogen bonded to amidic carbonyl of Asn132 via bridging water molecule (H_2O 60) through the amine NH of staurosporine and the carboxylic acid of 5'-Cl, respectively (Fig. 4C and 4D). Comparatively, the chlorobenzene of 5'-Cl stacks against the aromatic side chain of Phe82 (Fig. 4D) in a similar manner to π-stacking of one of the indolobenzenes of staurosporine against the same aromatic ring (Phe82, Fig. 4C). On the other hand, the other indolobenzene of staurosporine stacks between the aromatic ring of Phe80, the isopropyl of Val18 and the isobutyl of Leu134 (Fig. 4C), which is analogous to fitting the benzene ring of the quinolone system of 5'-Cl into the same boundaries (aromatic ring of Phe80, the isopropyl of Val18 and the isobutyl of Leu134). Accordingly, it can be safely concluded that both 5'-Cl and staurosporine bind and inhibit CDK2 kinase activity in similar fashion.

Table 1. Effect of 5'-Cl on cell cycle progression in different cancer cell lines after 48 h incubation. Results are expressed as the percentage of total cells. Data mean ± SD of triplicate independent experiments. *for statistically insignificant and ** for significant values

Cell Line	Cell Cycle Phases	Control	5.0 µM	10.0 µM	15.0 µM
K562	G0/G1	44.50 ± 0.73	54.46 ± 1.76 **	67.43 ± 3.46 **	74.07 ± 3.26 **
	S	23.42 ± 1.22	19.05 ± 0.95 **	13.81 ± 0.76 **	9.39 ± 0.69 **
	G2/M	21.60 ± 2.07	14.33 ± 1.83 **	8.47 ± 0.49 **	1.35 ± 1.49 **
THP-1	G0/G1	47.63 ± 0.98	56.42 ± 1.83 **	54.55 ± 3.34 **	40.96 ± 3.85 *
	S	17.42 ± 1.66	16.76 ± 0.91 *	16.84 ± 1.27 *	6.21 ± 1.27 **
	G2/M	27.60 ± 3.14	13.53 ± 2.73 **	15.11 ± 1.70 **	35.11 ± 3.61 **
HepG2	G0/G1	35.60 ± 2.06	36.22 ± 1.83 *	42.79 ± 2.09 **	49.66 ± 3.08 **
	S	17.00 ± 1.92	18.15 ± 2.49 *	17.59 ± 1.28 *	14.37 ± 0.76 **
	G2/M	37.26 ± 4.14	35.68 ± 3.72 *	22.63± 2.81 **	13.11 ± 4.71 **
MCF-7	G0/G1	33.31 ± 1.80	31.93 ± 2.70 *	39.58 ± 1.92 **	43.38 ± 2.57 **
	S	11.95 ± 0.62	13.03 ± 1.23 *	8.24 ± 0.72 **	6.22 ± 1.44 **
	G2/M	38.47 ± 3.04	37.47 ± 2.60 *	27.47 ± 3.67 **	20.75 ± 4.25 **
Caco-2	G0/G1	48.41 ± 2.34	49.30 ± 1.58 *	37.05 ± 1.58 **	26.31 ± 2.33 **
	S	8.95 ± 0.83	8.11 ± 0.69 *	7.69 ± 1.23 *	7.09 ± 1.23 *
	G2/M	36.98 ± 1.93	38.45 ± 2.37 *	43.86 ± 1.56 **	48.63 ± 3.52 **

Fig. 5 compares how a potent CDK4 inhibitor (PDB code: 1PU501) binds within the crystal structure of CDK4 that mimics CDK2 (PDB code: 1GIH, resolution 2.80 Å) with the way 5'-Cl docks into the binding pocket of the same protein. Incidentally, inactive CDK2 monomer is closely homologous to CDK4 and therefore was used as a structural surrogate for CDK4 [39]. This approach is convenient since the crystal structure of CDK2 is known, and the crystals are particularly robust, often diffract to high resolution and can readily be soaked in inhibitor solutions enabling rapid experimental support for molecular design strategies. The binding conformations obtained with CDK2 were interpreted assuming they were relevant to the true CDK4 target [40].

Fig. 5C and 5D show the similarity in the hydrogen bonding pattern of the central urea linker of co-crystallized 1PU501 and central 2-indolone of docked 5'-Cl structure to NH and carbonyl of Leu83. Similarly, the benzene ring of the dihydroisoindolone fragment of co-crystallized 1PU501 is fitted within a hydrophobic pouch composed of the side chains of Ala144, Val64 and Ala31 where it stacks against the aromatic ring of Phe80 (Fig. 5C). This interaction is closely homologous to fitting the chlorobenzene of 5'-Cl in the same pouch where the chlorobenzene ring stacks against the aromatic ring of Phe80 (Fig. 5D).

Similarly, the benzene ring of the quinolone system of 5'-Cl is fitted at close proximity to the isobutyl side chain of Ile10 (Fig. 5D) suggesting the existence of mutual hydrophobic interactions. This is analogous to positioning the pyridine ring of co-crystallized 1PU501 close to Ile10 isobutyl group (Fig. 5C) suggesting the existence of similar hydrophobic interactions.

Although 1PU501 is preferred over 5'-Cl with a hydrogen-bonding interaction connecting its dihydroisoindolone carbonyl group with the ammonium side chain of Lys33 (Fig. 5C), docked 5'-Cl is compensated with an extra hydrogen bonding interaction connecting its carboxylic acid moiety with Asp86 via bridging water molecule (H_2O39). Thus docking study suggests that 5'-Cl directly binds to the ATP binding site of the catalytic subunit of CDK2 and CDK4

Effect of 5'-Cl on cell cycle progression of other human cancer cell lines

We have recently shown that 5'-Cl inhibits the cell growth of various hematological and solid tumor cell lines including K562, THP-1, HepG2, MCF-7 and Caco-2 [29]. To determine whether the antiproliferative effect of 5'-Cl is associated with inhibition of cell cycle progression, these cells were treated with increasing concentrations of the compound (0.0 to 15.0 µM) for 48h and then analyzed for cell cycle phases. As shown in Table 1, 5'-Cl induced an increase in the percentage of G0/G1 phase in K562, HepG2 and MCF-7 in a dose-dependent manner with concomitant decrease in the G2/M and S phases ($p < 0.05$). In THP-1 cells, exposure to 5.0 µM and 10.0 µM of 5'-Cl induced cell cycle arrest at G1 ($p < 0.05$), while 15.0 µM of the compound significantly inhibited cell cycle at G2/M phase ($p < 0.05$). Interestingly, 5'-Cl induced only a dose-dependent inhibition of cell cycle at the G2/M phase

with concomitant decrease in the G0/G1 population in Caco-2 cells ($p < 0.05$). Incubation of all these cancer cell lines for 24h also gave similar results (data not shown). These data are in agreement with the previously shown cytotoxicity results [29], and suggest that antiproliferative effect of 5'-Cl towards various cancer cell lines is, at least in part, mediated by inhibition of cell cycle progression.

Discussion

Previous studies have shown that many isoindigo derivatives exhibit potent antitumor activity against several human and murine cancer cell lines [reviewed in [24]]. The antitumor properties of some of these compounds have been studied with respect to apoptosis and cell cycle arrest. Indirubin and several of its analogues exhibit their anticancer activity through modulating CDKs, which will arrest cell cycle progression leading to cell death by apoptosis [17-20, 22, 23, 25-28]. Multiple indirubin derivatives have been shown to arrest cell cycle at G0/G1 phase at low micromolar concentrations (up to 1 μM), while higher concentrations, ≥ 5 μM, inhibit cell cycle at G2/M phase [23]. Further increase in the concentrations of these compounds arrested cells at the sub-G1 phase indicating onset of apoptotic death in leukemia cells [23]. These compounds have been shown to inhibit the kinase activity of CDK1/cyclin B complex. Leclerc and coworkers have shown that the antiproliferative effect of indirubins is related to their ability to inhibit the kinase activity of GSK-3β, CDK1/cyclin B and CDK5/p25 [22]. Moon and coworkers [20] have synthesized novel indirubin analogs and shown that the antitumor activities are mediated by their ability to bind and inhibit the catalytic subunit of CDK2. Meisoindigo compounds have been demonstrated to induce apoptosis, arrest HT-29 colon cancer cells at G2/M phase, inhibit the activity of GSK-3β and effectively reduce tumor size in HT-29 cell xenograft nude mice model [19]. Natura™, meisoindigo and other related compounds have been demonstrated to induce apoptosis in various cancer cell lines and inhibit the activity of CDK4, leading to cell cycle arrest at the G0/G1 phase [41, 42]. The substituted 1-(β-d-glucopyranosyl)-isoindigo derivatives synthesized by Sassatelli and coworkers show strong antitumor activities towards a panel of human solid cancer cell lines (PC 3, DLD-1, MCF-7, M4Beu, A549, PA 1), but less effective in the noncancerous murine L929 and human fibroblast primary cultured cells [43]. These glycosyl-isoindigo derivatives strongly inhibit the CDK2/cyclin A kinase activity leading to G2/M cell cycle arrest [43]. Despite the progress in the synthesis of isoindigo derivatives and assessing their antiproliferative activities and mechanisms of action, the bioavailability and selectivity of this group of molecules towards tumor cells restrict their pharmacological application in cancer treatment.

Two compounds (5'-Cl and 5'-Br, with Chloro- and Bromo-substitution at the 5' position of benzo-ring E, respectively), of our newly synthesized group of pyridone-annelated isoindigo have an increased water solubility, and show strong antiproliferative activities in various hematological (K562 and THP-1) and solid tumor (HepG2, MCF-7 and Caco-2) cell lines at low concentrations, but not in noncancerous human (HEK-293) and murine (L-929) cells, suggesting their high efficacy and selectivity as antitumor agents [29]. In addition, these two compounds, but not 6'-Cl, 6'-Br or 5'-NO_2, induce a dose-dependent apoptosis in the chronic myelogenous leukemia cell line K562, suggesting the critical role of substitution at the 5'-position of benzo-ring E in controlling the antiproliferative activities of this group of compounds [29]. In a more recent study, we have shown that the 5'-Cl compound efficiently inhibits the growth of HL-60 cells (IC_{50} 4.27 ± 0.40 μM) by inducing a dose and time-dependent apoptosis in treated cells. Our results show that the compound triggers both caspase-dependent and caspase-independent apoptosis and dysfunctioning of mitochondria in HL-60 treated cells [30]. These results indicate that 5'-Cl is a promising potential therapeutic agent for myelogenous leukemia. However, this molecule deserve further investigation to elucidate its detailed molecular mechanism of antiproliferative activities.

Several studies have shown that isoindigo derivatives block cell cycle progression at the G0/G1 or G2/M phase depending on the cell type and type of drugs [17]. Here we show that 5'-Cl inhibits cell cycle progression and induces cell cycle arrest in the G0/G1 phase of HL-60 cells both in a dose and time-dependent manner. The compound also inhibits G0/G1 cell cycle progression in K562, THP-1, HepG2 and MCF-7 cell lines. Interestingly, 5'-Cl shows a dose-dependent accumulation of G2/M population in Caco-2 cells, and at high concentrations of 20 μM in THP-1 cells. This suggests that the targeted CDK/cyclin complexes by 5'-Cl may vary in different cancer cell lines.

Cell cycle progression in eukaryotes is controlled by protein kinase complexes consisting of CDK and their associated cyclins. During G1-phase progression, the complexes CDK2/cyclin E, CDK4/cyclin D and CDK6/cyclin D are activated to promote cell cycle transition from the G1 to the S phase. We found that D-type cyclins (D1, D2 and D3), CDK2 and CDK4 are significantly down-regulated in HL-60 cells after treatment with 5'-Cl. On the other hand, the expression patterns of cyclin E, cyclin A (data not shown) and CDK6 were not significantly altered after exposure to various doses of the compound. This finding suggests that inhibiting the expression of cyclin D, CDK2 and CDK4 are involved in 5'-Cl-induced cell cycle arrest at G0/G1 phase.

Phosphorylation of the retinoblastoma protein Rb is critically controlled during G1-S progression [7, 8]. Rb is phosphorylated by CDK2/cyclin E, CDK4/cyclin D and CDK6/cyclin D complexes [8-10]. Hyperphosphorylation of Rb leads to dissociation of the transcription factors E2F from this protein, which subsequently, activates transcription of the components of the DNA replication machinery, and thereby committing the cell to S phase of the cell cycle. We found that, the expression level of Rb is not affected in 5'-Cl-treated HL-60 cells, whereas the level of the phosphorylated form of Rb decreases significantly in a dose-dependent manner, indicating that 5'-Cl can suppress the phosphorylation of this protein.

The activity of CDK/cyclin complexes is inhibited by binding of CKI. The CKI p21 associates with and inhibits the activity of CDK2/cyclin E complex, thereby causing a hypophosphorylation of Rb and arresting cell cycle at G0/G1 [5]. Our results show that 5'-Cl induces a dose-dependent increase in p21 which might lead to a reduction in the phosphorylation of Rb. However, HL-60 and several other cancer cell lines are deficient in functional p53 [14, 44, 45], suggesting that 5'-Cl-induced up-regulation of p21 is controlled *via* a p53-independent mechanism.

Indirubin and isoindigo derivatives have been shown to inhibit different CDKs by competing with ATP binding at the catalytic site, leading to cell cycle arrest in G0/G1 or G2/M phase depending on the drug structure [17]. Docking studies presented here suggest that 5'-Cl directly binds to the ATP binding site of the catalytic subunit of CDK2 and CDK4. Indeed, the compound exhibits a concentration-dependent inhibitory effect on CDK2 and CDK4, obtained from untreated HL-60. The kinase activities of CDK2 and CDK4 are also inhibited in a dose and time-dependent manner in HL-60 treated cells. The CDK2 and CDK4 inhibition due to these direct and indirect actions leads to hypophosphorylation of Rb in the 5'-Cl treated cells. However, activation of CDKs is also controlled by phosphorylation at some of their conserved amino acid residues [46]. It is therefore possible that 5'-Cl inhibits the CDK activating kinases (CAKs) or activates the CDK-inactivating phosphatases, which are regulators for CDKs function. Therefore, additional studies are needed to determine whether the inhibition of CAKs or activation of CDK-inactivating phosphatases contributes to the inhibition of the kinase activity of CDK2 and CDK4. In addition, CDK6 can also phosphorylate Rb within cells. The question of whether or not 5'-Cl directly inhibits CDK6 activity remain to be answered. furthermore, although down-regulation of D-type cyclins by 5'-Cl suggests that it is the main causative effect for inhibiting the CDK4 kinase activity, we cannot rule out the possibility that the test compound may block cyclin D binding to CDK4, or binding of other cyclins to their specific CDKs, thereby inhibiting CDK4/cyclin D complex activity.

In conclusion, our results show that 5'-Cl arrests cell cycle at G0/G1 through its direct binding to the catalytic subunit of CDK2 and CDK4 and indirectly by modulating the expression of the two CDKs, cyclin D and p21. Recently, we have also shown that the growth

inhibitory effect of 5'-Cl is also mediated by its ability to induce a caspase-dependent and caspase-independent apoptosis and deregulating the mitochondria functions. Together, these data indicate that the antiproliferative activities of 5'-Cl is mediated by apoptosis and inhibition of cell cycle progression. The findings that 5'-Cl has a higher water solubility than the other reported isoindigos, and its ability to selectively induce apoptosis and cell cycle arrest in various cancer cell lines, but not in noncancerous cells at low exposure doses, strongly nominate this compound as a chemotherapeutic candidate. Therefore, further detailed characterization of the antitumor mechanisms of this compound both *in vitro* and *in vivo* are essential for its pharmacological application in cancer treatment.

Acknowledgments

This project is supported by a research grant from King Abdulaziz City for Science and Technology (KACST; Grant number- AT-34-136 Riyadh, Kingdom of Saudi Arabia) for Saleh AM. El-Abadelah MM is supported by the Scientific Research Support Fund (SRSF/project number- mph/1/6/2011, Amman, Jordan). Publication cost is supported by King Abdullah International Medical Research Center (KAIMRC) in Riyadh, Saudi Arabia.

Disclosure Statement

The authors declare no conflict of interest.

References

1 Schnerch D, Yalcintepe J, Schmidts A, Becker H, Follo M, Engelhardt M, Wasch R: Cell cycle control in acute myeloid leukemia. Am J Cancer Res 2012;2:508-528.
2 Sherr CJ: Cell cycle control and cancer. Harvey Lect 2000;96:73-92.
3 Pavletich NP: Mechanisms of cyclin-dependent kinase regulation: structures of Cdks, their cyclin activators, and Cip and INK4 inhibitors. J Mol Biol 1999;287:821-828.
4 Lim S, Kaldis P: Cdks, cyclins and CKIs: roles beyond cell cycle regulation. Development 2013;140:3079-3093.
5 Vidal A, Koff A: Cell-cycle inhibitors: three families united by a common cause. Gene 2000;247:1-15.
6 Gali-Muhtasib H, Bakkar N: Modulating cell cycle: current applications and prospects for future drug development. Curr Cancer Drug Targets 2002;2:309-336.
7 Taya Y: RB kinases and RB-binding proteins: new points of view. Trends Biochem Sci 1997;22:14-17.
8 Weinberg RA: The retinoblastoma protein and cell cycle control. Cell 1995;81:323-330.
9 Botz J, Zerfass-Thome K, Spitkovsky D, Delius H, Vogt B, Eilers M, Hatzigeorgiou A, Jansen-Durr P: Cell cycle regulation of the murine cyclin E gene depends on an E2F binding site in the promoter. Mol Cell Biol 1996;16:3401-3409.
10 Muller H, Helin K: The E2F transcription factors: key regulators of cell proliferation. Biochim Biophys Acta 2000;1470:M1-12.
11 El-Deiry WS, Harper JW, O'Connor PM, Velculescu VE, Canman CE, Jackman J, Pietenpol JA, Burrell M, Hill DE, Wang Y, et al.: WAF1/CIP1 is induced in p53-mediated G1 arrest and apoptosis. Cancer Res 1994;54:1169-1174.
12 El-Deiry WS, Tokino T, Velculescu VE, Levy DB, Parsons R, Trent JM, Lin D, Mercer WE, Kinzler KW, Vogelstein B: WAF1, a potential mediator of p53 tumor suppression. Cell 1993;75:817-825.
13 Levine AJ: p53, the cellular gatekeeper for growth and division. Cell 1997;88:323-331.
14 Parker SB, Eichele G, Zhang P, Rawls A, Sands AT, Bradley A, Olson EN, Harper JW, Elledge SJ: p53-independent expression of p21Cip1 in muscle and other terminally differentiating cells. Science 1995;267:1024-1027.

15 Polychronopoulos P, Magiatis P, Skaltsounis AL, Myrianthopoulos V, Mikros E, Tarricone A, Musacchio A, Roe SM, Pearl L, Leost M, Greengard P, Meijer L: Structural basis for the synthesis of indirubins as potent and selective inhibitors of glycogen synthase kinase-3 and cyclin-dependent kinases. J Med Chem 2004;47:935-946.

16 Wu GY, Fang FD: Studies on the mechanism of indirubin action in the treatment of chronic granulocytic leukemia. II. Effects of indirubin on nucleic acid and protein synthesis in animal transplantable tumor cells and normal proliferating cells in vitro (author's transl). Zhongguo Yi Xue Ke Xue Yuan Xue Bao 1980;2:83-87.

17 Xiao Z, Hao Y, Liu B, Qian L: Indirubin and meisoindigo in the treatment of chronic myelogenous leukemia in China. Leuk Lymphoma 2002;43:1763-1768.

18 Liu XM, Wang LG, Li HY, Ji XJ: Induction of differentiation and down-regulation of c-myb gene expression in ML-1 human myeloblastic leukemia cells by the clinically effective anti-leukemia agent meisoindigo. Biochem Pharmacol 1996;51:1545-1551.

19 Mingxin Z, Yan L, Hongbo W, Jianhua Z, Hongyan L, He L, Hongqi X, Sen Z, Xiaoguang C: The antitumor activity of meisoindigo against human colorectal cancer HT-29 cells in vitro and in vivo. J Chemother 2008;20:728-733.

20 Moon MJ, Lee SK, Lee JW, Song WK, Kim SW, Kim JI, Cho C, Choi SJ, Kim YC: Synthesis and structure-activity relationships of novel indirubin derivatives as potent anti-proliferative agents with CDK2 inhibitory activities. Bioorg Med Chem 2006;14:237-246.

21 Wu GY, Liu JZ, Fang FD, Zuo J: Studies on the mechanism of indirubin action in the treatment of chronic granulocytic leukemia. V. Binding between indirubin and DNA and identification of the type of binding. Sci Sin B 1982;25:1071-1079.

22 Leclerc S, Garnier M, Hoessel R, Marko D, Bibb JA, Snyder GL, Greengard P, Biernat J, Wu YZ, Mandelkow EM, Eisenbrand G, Meijer L: Indirubins inhibit glycogen synthase kinase-3 beta and CDK5/p25, two protein kinases involved in abnormal tau phosphorylation in Alzheimer's disease. A property common to most cyclin-dependent kinase inhibitors? J Biol Chem 2001;276:251-260.

23 Marko D, Schatzle S, Friedel A, Genzlinger A, Zankl H, Meijer L, Eisenbrand G: Inhibition of cyclin-dependent kinase 1 (CDK1) by indirubin derivatives in human tumour cells. Br J Cancer 2001;84:283-289.

24 Xiao Z, Wang Y, Lu L, Li Z, Peng Z, Han Z, Hao Y: Anti-angiogenesis effects of meisoindigo on chronic myelogenous leukemia in vitro. Leuk Res 2006;30:54-59.

25 Du DJ, Ceng QT: Effect of indirubin on the incorporation of isotope labeled precursors into nucleic acid and protein of tumor tissues. Chinese Trad Herb Drugs 1981;12:406- 409.

26 Ji XJ, Zhang FR, Liu Y, Gu QM: Studies on the antineoplastic action of N-methylisoindigotin. Yao Xue Xue Bao 1985;20:247-251.

27 Sassatelli M, Bouchikhi F, Messaoudi S, Anizon F, Debiton E, Barthomeuf C, Prudhomme M, Moreau P: Synthesis and antiproliferative activities of diversely substituted glycosyl-isoindigo derivatives. Eur J Med Chem 2006;41:88-100.

28 Zhao P, Li Y, Gao G, Wang S, Yan Y, Zhan X, Liu Z, Mao Z, Chen S, Wang L: Design, synthesis and biological evaluation of N-alkyl or aryl substituted isoindigo derivatives as potential dual cyclin-dependent kinase 2 (CDK2)/glycogen synthase kinase 3beta (GSK-3beta) phosphorylation inhibitors. Eur J Med Chem 2014;86:165-174.

29 Saleh AM, Al-As'ad RM, El-Abadelah MM, Sabri SS, Zahra JA, Alaskar AS, Aljada A: Synthesis and biological evaluation of new pyridone-annelated isoindigos as anti-proliferative agents. Molecules 2014;19:13076-13092.

30 Saleh AM, Aljada A, El-Abadelah MM, Sabri SS, Zahra JA, Nasr A, Aziz MA: The Pyridone-Annelated Isoindigo (5'-Cl) Induces Apoptosis, Dysregulation of Mitochondria and Formation of ROS in Leukemic HL-60 Cells. Cell Physiol Biochem 2015;35:1958-1974.

31 Li L, Dai HJ, Ye M, Wang SL, Xiao XJ, Zheng J, Chen HY, Luo YH, Liu J: Lycorine induces cell-cycle arrest in the G0/G1 phase in K562 cells via HDAC inhibition. Cancer Cell Int 2012;12:49.

32 Miliani de Marval PL, Macias E, Rounbehler R, Sicinski P, Kiyokawa H, Johnson DG, Conti CJ, Rodriguez-Puebla ML: Lack of cyclin-dependent kinase 4 inhibits c-myc tumorigenic activities in epithelial tissues. Mol Cell Biol 2004;24:7538-7547.

33 Pan MH, Chen WJ, Lin-Shiau SY, Ho CT, Lin JK: Tangeretin induces cell-cycle G1 arrest through inhibiting cyclin-dependent kinases 2 and 4 activities as well as elevating Cdk inhibitors p21 and p27 in human colorectal carcinoma cells. Carcinogenesis 2002;23:1677-1684.
34 Ramsey MR, Krishnamurthy J, Pei XH, Torrice C, Lin W, Carrasco DR, Ligon KL, Xiong Y, Sharpless NE: Expression of p16Ink4a compensates for p18Ink4c loss in cyclin-dependent kinase 4/6-dependent tumors and tissues. Cancer Res 2007;67:4732-4741.
35 Gasteiger J, Marsili M: Iterative partial equalization of orbital electronegativity—a rapid access to atomic charges. Tetrahedron 1980;36:3219- 3228.
36 Gehlhaar DK, Verkhivker GM, Rejto PA, Sherman CJ, Fogel DB, Fogel LJ, Freer ST: Molecular recognition of the inhibitor AG-1343 by HIV-1 protease: conformationally flexible docking by evolutionary programming. Chem Biol 1995;2:317-324.
37 Venkatachalam CM, Jiang X, Oldfield T, Waldman M: LigandFit: a novel method for the shape-directed rapid docking of ligands to protein active sites. J Mol Graph Model 2003;21:289-307.
38 Hauck L, von Harsdorf R: E2F transcription factors and pRb pocket proteins in cell cycle progression. Methods Mol Biol 2005;296:239-245.
39 Kawanishi N, Sugimoto T, Shibata J, Nakamura K, Masutani K, Ikuta M, Hirai H: Structure-based drug design of a highly potent CDK1,2,4,6 inhibitor with novel macrocyclic quinoxalin-2-one structure. Bioorg Med Chem Lett 2006;16:5122-5126.
40 Beattie JF, Breault GA, Ellston RP, Green S, Jewsbury PJ, Midgley CJ, Naven RT, Minshull CA, Pauptit RA, Tucker JA, Pease JE: Cyclin-dependent kinase 4 inhibitors as a treatment for cancer. Part 1: identification and optimisation of substituted 4,6-bis anilino pyrimidines. Bioorg Med Chem Lett 2003;13:2955-2960.
41 Wang L, Liu X, Chen R: Derivatives of isoindigo, indigo and indirubin and methods of treating cancer. United States Patent. US 6,933,315 B2 2003.
42 Wang L, Liu X, Chen R: Derivatives of isoindigo, indigo and indirubin and use in treating cancer. WO Patent. WO 03/051900 A1 2003.
43 Sassatelli M, Bouchikhi F, Aboab B, Anizon F, Fabbro D, Prudhomme M, Moreau P: In-vitro antiproliferative activities and kinase inhibitory potencies of glycosyl-isoindigo derivatives. Anticancer Drugs 2007;18:1069-1074.
44 Livingstone LR, White A, Sprouse J, Livanos E, Jacks T, Tlsty TD: Altered cell cycle arrest and gene amplification potential accompany loss of wild-type p53. Cell 1992;70:923-935.
45 Yin Y, Tainsky MA, Bischoff FZ, Strong LC, Wahl GM: Wild-type p53 restores cell cycle control and inhibits gene amplification in cells with mutant p53 alleles. Cell 1992;70:937-948.
46 Morgan DO: Principles of CDK regulation. Nature 1995;374:131-134.